LINEAR RESISTANCE LIMITING THE CURRENT OF INTERGRANULAR BARRIERS IN VARISTOR CERAMICS

A. I. Ivon

Oles Honchar Dnipro National University, Dnipro, Ukraine
e-mail: aii_vel93@i.ua

Method for measuring the linear resistivity ρ_{lin}, which affects the volt-ampere characteristic (VAC) nonlinearity of varistor materials in a high current region is proposed. For ZnO based varistor ceramics the dependence of ρ_{lin} on amplitude density J_{max} of current pulse is studied in the range 5 A·cm^{-2} – 4600 A·cm^{-2}. At J_{max}< 200 A·cm^{-2} a sharp decrease of ρ_{lin} with increasing J_{max} takes place. This behavior indicates a non-uniform distribution of high current over the cross section of ceramics sample. At J_{max} > 1000 A·cm^{-2} ρ_{lin} does not depend on J_{max} and has a value of 0.49 – 0.50 Ohm·cm corresponding to the volume resistivity ρ_g of ZnO grains. The decrease in nonlinearity of VAC at high currents is due to the formation of conductive paths of electric current between the electrodes of a sample. Along such paths, all intergranular double Schottky barriers are in a reversible electrical breakdown mode, probably due to impact ionization. The current in these paths is limited by small linear volume resistance of the grains. A spread of grain sizes is the reason for existence of current paths with different numbers of contacts between grains and therefore with different breakdown voltages. At voltage increases, the sequential formation of parallel-connected conductive paths occurs. This explains the inhomogeneous distribution of high current over the cross section of a sample at J_{max} < 200 A·cm^{-2}. At J_{max} > 1000 A·cm^{-2} almost all current paths in a sample are switched on and the value of ρ_{lin} limiting the barriers current is close to the volume resistivity ρ_g of grains.

Keywords: electroceramics, non-linear conductivity, grain boundaries, varistor.

Received 25.10.2023; Received in revised form 12.11.2023; Accepted 15.11.2023

1. Introduction

ZnO based ceramics with small additions of other oxides have a high nonlinearity of volt-ampere characteristic (VAC) and widely used for making varistors [1]. The surge arresters for power transmission circuits are created based on varistors. Varistors are widely used in electronics to protect from overvoltages. Surge protection effectiveness is determined by the clamp ratio U_I/U_{I0} (U_{I0} is the voltage at current $I_0 \sim 10^{-4}$ A, U_I is the voltage at electrical overvoltage pulse presence). Effectiveness of surge protection is greater when the clamp ratio is closer to unity. The typical clamp ratio for ZnO based varistors is about 1.41 at the current of 100 A and about 1.76 at the current of 1000 A [2]. The reason for the increase in U_I/U_{I0} with increasing of overvoltage current I is the decrease of VAC nonlinearity.

The high nonlinearity of the volt-ampere characteristic for ZnO based ceramics is associated with the intergranular double Schottky barriers that arise in the contact region of ZnO grains due to the capture of electrons from the bulk of grains on the surface states [1]. As a result, thin near-surface layers depleted in charge carriers are formed in the contact region of ZnO grains. These layers have an ohmic resistance of about 10^{-13} Ohm. Their resistance sharply decreases with increases of voltage due to the high nonlinearity of VAC for the double Schottky barrier. When the resistance of near-surface layers of ZnO grains becomes close to their volume resistance, this linear volume resistance limits the electrical current of barriers and the nonlinearity of volt-ampere characteristic decreases.

Thus, the linear resistance associated with the volume electrical resistance of varistor ceramics grains has a direct effect on the clamp ratio U_I/U_{I0}. Therefore, control of linear resistance, which determines the nonlinear properties of varistor materials at high electric currents, is an urgent task.

The aim of this work is to develop a methodology for measuring the linear resistivity ρ_{lin} limiting the current of intergranular barriers in varistor ceramics and to study this resistivity at high currents for ZnO based varistor ceramics.

2. Materials and methods

The microstructure of varistor ceramics based on ZnO [1] and SnO_2 [3] consists of oxide grains with high volume electrical conductivity. In the grain contact zone during ceramic sintering, subsurface layers with the double Schottky barriers having a low ohmic conductivity are formed.

Taking into account the microstructure of varistor ceramics, we can use the equivalent circuit shown in Fig. 1a to describe its electrical properties. Here *Rlin* is the effective linear resistance determined by the volume electrical conductivity of ZnO (SnO_2) grains. The effective capacitance *Cb* associated with grain contact determines the reactive component of current I_{Cb} in ceramics sample. The effective non-linear resistance *Rb* determines the active component of current I_{Rb}. This resistance is related to VAC of the double Schottky barrier.

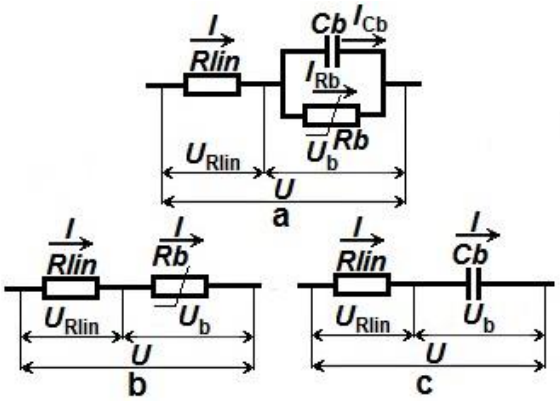

Fig. 1. Equivalent circuits of varistor ceramics sample: a - initial circuit; b – circuit when the current $I_{Rb} >> I_{Cb}$, c - circuit when the current $I_{Cb} >> I_{Rb}$

It follows from the equivalent circuit in Fig. 1a that the voltage U and the current I of the varistor ceramics sample are determined by the relations:

$$U = U_{Rlin} + U_b \quad (1)$$

$$I = I_{Cb} + I_{Rb}. \quad (2)$$

Taking into account that $U_{Rlin} = I \cdot Rlin$, the equation (1) can be represented as

$$U = I \cdot Rlin + U_b \quad (3)$$

It follows from the equation (3), the differential resistance $R_{dif} = dU/dI$ is determined as

$$R_{dif} = Rlin + dU_b/dI. \quad (4)$$

As it can be seen, the effective linear resistance *Rlin* associated with the volume electrical conductivity of ceramics grains contributes to R_{dif}. As shown in [4, 5], this makes it possible to use R_{dif} for determining the volume electrical resistivity ρ_{lin} of ZnO and SnO_2 grains in varistor materials.

Resistance *Rlin* makes the largest contribution to R_{dif} in the region of high electric currents. Therefore, to determine *Rlin*, it is necessary to use the volt-ampere characteristic of varistor ceramics sample measured at high electric currents. To exclude the thermal breakdown of a sample upon registration of VAC, one can use the single exponential voltage pulses $U = U_0 \exp(-t/\tau)$ (U_0 is the pulse amplitude, t is the time, τ is the time constant).

The dependence of active electric current I_{Rb} on voltage U_b applied in the contact zone of grains with double Schottky barrier can be approximated by the well-known formula [1]:

$$I_{\mathrm{Rb}} = BU_{\mathrm{b}}^{\alpha}, \tag{5}$$

where B is a constant, α is the nonlinearity coefficient ($\alpha \sim 50$ for ZnO based varistors).

The reactive electric current I_{Cb} is described by the equation

$$I_{\mathrm{Cb}} = Cb\frac{dU_{\mathrm{b}}}{dt}\ . \tag{6}$$

In moment of application the single voltage pulse to a sample ($t = 0$), the capacitance Cb in discharged state ($U_{\mathrm{b}} = 0$). Therefore, according (5), the current $I_{\mathrm{Rb}} = 0$. The current I is completely determined by the capacitive current I_{Cb}. During the charging of Cb, the current I_{Cb} decreases, and the current I_{Rb} increases due to an increase of U_{b}. For the exponential voltage pulse with $\tau >> \tau_{\mathrm{b}}$ ($\tau_{\mathrm{b}} = CbRlin$), it should be expected that after some time the active current I_{Rb} will make the main contribution to current I. Therefore, in oscillogram of the current pulse two time intervals can be distinguished, in which $I_{\mathrm{Cb}} >> I_{\mathrm{Rb}}$ and $I_{\mathrm{Rb}} >> I_{\mathrm{Cb}}$. First interval corresponds to beginning of current pulse, second to its end. In the time interval where $I_{\mathrm{Cb}} >> I_{\mathrm{Rb}}$, one can take $I = I_{\mathrm{Cb}}$ and use the circuit shown in Fig. 1c. In the time interval where $I_{\mathrm{Rb}} >> I_{\mathrm{Cb}}$, one can take $I = I_{\mathrm{Rb}}$ and use the circuit shown in Fig. 1b.

Let us analyze the dependence of resistance R_{dif} on current I in both time intervals.

According to (5) at $I = I_{\mathrm{Rb}}$ the voltage applying to intergranular barriers is $U_{\mathrm{b}} = AI^{1/\alpha}$, where $A = B^{-1/\alpha}$. Therefore, the equation (3) can be represented as

$$U = I \cdot Rlin + AI^{\frac{1}{\alpha}}. \tag{7}$$

It follows from (7), that in the case when $I_{\mathrm{Rb}} >> I_{\mathrm{Cb}}$, the dependence of differential resistance $R_{\mathrm{dif}} = dU/dI$ on current I is determined by the relation

$$R_{\mathrm{dif}} = Rlin + \frac{A}{\alpha} I^{\frac{1}{\alpha}-1}.$$

Since $1/\alpha << 1$, this relation can be written as

$$R_{\mathrm{dif}} = Rlin + \frac{A}{\alpha}\frac{1}{I}.$$

If a sample has the thickness L and the electrodes area S, then we can obtain the last equation in specific parameters:

$$\rho_{\mathrm{dif}} = \rho_{\mathrm{lin}} + \frac{A}{\alpha L}\frac{1}{J}. \tag{8}$$

It follows from the equation (8), at current $I = I_{\mathrm{Rb}}$ the linear dependence of differential resistivity ρ_{dif} on reverse current density J^{-1} takes place. This makes it possible to determine the value of ρ_{lin} by extrapolating linear dependence $\rho_{\mathrm{dif}}(J^{-1})$ to the value $J^{-1} = 0$.

In the time interval corresponding to the beginning of current pulse $I_{\mathrm{Cb}} >> I_{\mathrm{Rb}}$ ($I = I_{\mathrm{Cb}}$). Therefore, it is necessary to use the equivalent scheme in fig. 1c. Taking into account this scheme and the exponential shape of voltage pulse $U = U_0\exp(-t/\tau)$ we can obtain on the basis of (3) and (6) the following equation:

$$-\frac{U_0}{Rlin\,\tau}\exp\left(-\frac{t}{\tau}\right) = \frac{dI}{dt} + \frac{I}{\tau_{\mathrm{b}}}, \tag{9}$$

where the time constant $\tau_{\mathrm{b}} = CbRlin$.

The solution of equation (9) under the initial conditions $t = 0$; $I = U_0/Rlin$ is

$$I = \frac{U_0}{Rlin(\gamma-1)}(\gamma\exp(-\frac{t}{\tau_b}) - \exp(-\frac{t}{\tau})), \quad (10)$$

where $\gamma = \tau/\tau_b$.

Using (10) and given that the voltage U_b is related to the current I as $U_b = \frac{1}{C_b}\int Idt$ the following expression can be obtained:

$$U_b = \frac{U_0\gamma}{(\gamma-1)}(\exp(-\frac{t}{\tau}) - \exp(-\frac{t}{\tau_b})). \quad (11)$$

From (11) it follows that after a time $t \geq 3\tau_b$, when $\tau >> \tau_b$ ($\gamma >> 1$), the voltage drop U_b across intergranular barriers is described by the relation $U_b \approx U_0\exp(-t/\tau)$, i. e. practically coincides with the voltage applied to a sample.

For the circuit in fig. 1c may be obtained the dependence $I = f(U)$ at $U = U_0\exp(-t/\tau)$. Take in account $t = \tau\ln(U_0/U)$ and the equation (11), an expression for dynamic volt-ampere characteristic related to the charge of the equivalent capacitance Cb may be obtained:

$$I = \frac{U_0}{R_g(\gamma-1)}\left(\gamma\left(\frac{U}{U_0}\right)^{\gamma} - \frac{U}{U_0}\right). \quad (12)$$

Since $\gamma >> 1$, the formula (12) can be represented as

$$I = \frac{U_0}{Rlin}\left(\frac{U}{U_0}\right)^{\gamma} \quad (13)$$

Thus, in the time intervals corresponding to the beginning ($I_{Cb} >> I_{Rb}$) and the end ($I_{Rb} >> I_{Cb}$) of current pulse, there is a nonlinear relationship between current I and voltage U with a high nonlinearity coefficient $\gamma >> 1$. Therefore, it is to be expected a linear relationship (8) between the differential resistivity ρ_{dif} and the inverse current density J^{-1} in entire interval of the current pulse. This makes it possible to determine the resistivity ρ_{lin} by extrapolating the dependence $\rho_{dif}(J^{-1})$ to $J^{-1} = 0$ for small sections selected on the oscillogram of current pulse. By measuring the differential resistivity ρ_{lin} for different sections of the current pulse oscillogram, we can get the dependence of ρ_{lin} on average current density J_{av} in these sections.

For measuring the differential resistivity ρ_{dif}, the raster images of analog oscillograms of voltage and current pulses were used. These images were obtained by photographing the analog storage oscilloscope screen with a digital camera. The raster images of calibration signal oscillograms were obtained with the same amplification and sweep. These images were used to define the scale of the oscillogram raster images. The instantaneous voltages and currents were measured using the scale of raster images, the coordinates of zero lines, and the coordinates of lines for impulse signals. The relative measurement error did not exceed ±1% since the absolute error at scanning of coordinates is ±1 pixel [6].

The software used in this work to measure the value of differential resistivity ρ_{dif} is described in [7]. This value was determined based on the scanning data of raster images of oscillograms for voltage and current pulses. Such oscillograms are schematically shown in Fig. 2. The program provides coordinate scanning in three points of the oscillogram raster image for voltage pulse (curve 1 in Fig. 2) and coordinates in corresponding points for

current pulse (curve 2 in Fig. 2). Then program calculates the instantaneous voltages U_1, U_2, U_3 and the instantaneous currents I_1, I_2, I_3 with using scanning data, the scale of raster images, and coordinates of zero voltage and current. Based on these data, the electric field strengths $E = U/L$ and the electric current densities $J = I/S$ are determined. Differential resistivity ρ_{dif} is calculated by the line $E = E_0 + \rho_{dif}J$ drawn across the above-mentioned points of volt-ampere characteristic using the least square method. The average electric current density J in the specified area of volt-ampere characteristic and its reciprocal value J^{-1} were calculated using the coordinates of three points in raster image of the current pulse oscillogram and the area of electrodes S. The electrodes with small area were used to provide high current density.

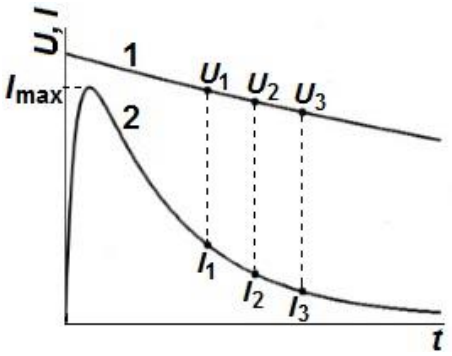

Fig. 2. Schematic image of voltage *U* (1) and current *I* (2) pulses oscillograms when the single exponential pulse of voltage is applied to varistor ceramics sample

At measuring resistivity ρ_{dif}, the x, y coordinates in three points of oscillograms raster image have scanned with the step of 100 pixels along the X axis (the time axis of oscillogram). The values of ρ_{dif} for different area in the raster image of voltage and current pulse were measured with a step of 50 pixels. The eight values of ρ_{dif} and their corresponding reciprocal values J^{-1} were used for dependence $\rho_{dif}(J^{-1})$ appropriate to a small sections of VAC. Such dependence obtained for ZnO based ceramics is shown in Fig. 3. As can be seen, this dependence is linear in accordance with the equation (8). The simple linear regression for drawing the line $\rho_{dif} = a + b/J$ through the points of dependence $\rho_{dif}(J^{-1})$ was used. In accordance with (8), the value of a for this line determines the linear resistivity ρ_{lin}. Based on the current density J at different values of ρ_{dif}, the average current density J_{av} was determined for section of VAC where thethemeasurement of ρ_{lin} was performed.

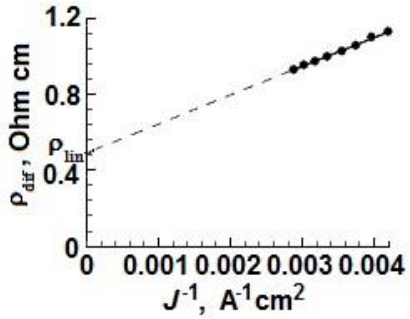

Fig. 3. Dependence of differential resistivity ρ_{dif} of ZnO based varistor ceramics on inverse current density J^{-1}. The measurement was made at average current density J_{av} = 292 A cm^{-2} and amplitude of current pulse J_{max} = 2390 A cm^{-2}. Temperature 298 K, ρ_{lin} = 0.49 Ohm cm, time constant τ 130 μs.

The resistivity ρ_{lin} limiting the current of intergranular barriers in ZnO based varistor ceramics was studied. The samples were prepared from the commercial ZnO based varistors (CH2-1, Russia). Such varistors material contains 97 mol.% ZnO and oxides Bi_2O_3, Sb_2O_3,

Co_3O_4, Cr_2O_3, MnO_2 as additions. Fabrication details of the samples with the small area of Ag electrodes (0.023 – 0.030 cm^2) are described in [4]. The area of electrodes was measured with relative error ±2% using the raster image of varistor surface with electrodes [8].

Oscillograms of the voltage and current pulses were recorded by C8-11 two-beam storage analog oscilloscope. Current was recorded as a voltage drop across the precision resistor of 1 Ohm connected in series with the sample. Single exponential voltage pulses (τ = 130 μs) obtained by the circuit described in [5] were used for measurements.

Raster images of voltage and current oscillograms, as well as oscillograms of calibration signals, were obtained using OLYMPUS C-765 digital camera with a resolution of 2288×1712 pixels. The relative measurement error of resistivity ρ_{lin} according to scanning data of oscillograms raster images is no more than ± 2%.

3. Results and discussion

Fig. 4 shows the dependences of resistivity ρ_{lin} limiting the current of intergranular barriers in ZnO based varistor ceramics on average current density J_{av}. These dependences were measured at the different current pulse amplitudes.

Two areas can be distinguished in the dependences $\rho_{lin}(J_{av})$. The area where ρ_{lin} is independent of J_{av} and the area where ρ_{lin} depends on J_{av}. The first area corresponds to low values of average current density J_{av} (the end of current pulse). The second area corresponds to large values of J_{av} (the beginning of current pulse).

In the time interval close to the end of the current pulse, the active current exceeds the reactive current of intergranular barriers $I_{Rb} >> I_{Cb}$. In this region, the active current I_{Rb} makes the main contribution to the current through the sample. It is determined by the static volt-ampere characteristic approximated by the formula (5). In the time interval close to the beginning of the current pulse, the reactive current I_{Cb} exceeds the active current $I_{Cb} >> I_{Rb}$. In this region, the reactive current I_{Cb} makes the main contribution to the electric current of varistor ceramics sample. This contribution described by the formulas (12) and (13) is determined by the dynamic volt-ampere characteristic of the effective barrier capacitance *Cb*.

As can be seen in Fig. 4, in the gentle slope section of dependence $\rho_{lin}(J_{av})$ the value of resistivity ρ_{lin} decreases with the current pulse amplitude J_{max} increasing. This allows us to conclude that the linear resistivity ρ_{lin} limiting the current of intergranular barriers is determined by the current pulse amplitude.

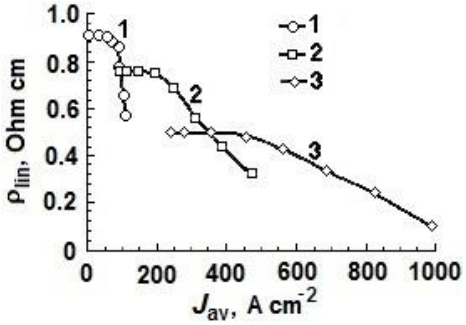

Fig. 4. Dependences of the resistivity ρ_{lin} on the current density J_{av}. Amplitude density of current pulse J_{max}, A cm^{-2}: 1 – 267; 2 – 936; 3 – 1500. The time constant for voltage pulse τ = 130 μs.

Measurements of ρ_{lin} dependence on the value of J_{max} were performed in the areas of the oscillogram raster images located close to the end of current pulse. For these areas $I_{Rb} >> I_{Cb}$. In this case the current I_{Rb} is determined by the static VAC of the intergranular double Schottky barriers. The dependence of resistivity ρ_{lin} on amplitude J_{max} is shown in Fig. 5.

As can be seen, in the interval J_{max} < 200 A cm^{-2} the resistivity ρ_{lin} rapidly decreases with J_{max} increasing and weakly depends on J_{max} in the interval J_{max} > 1000 A cm^{-2}.

The resistivity ρ_{lin} limiting the current of intergranular barriers in varistor ceramics is determined by the volume electric resistivity of grains ρ_g. Therefore, the dependence in Fig. 5 indicates a non-uniform distribution of high electric current across the sample section *S* when J_{max} < 200 A cm^{-2}. In this case the resistivity ρ_{lin} is the volume electric resistivity of grains ρ_g averaged over the sample cross-sectional area (the area of the electrodes) *S*.

If at a given amplitude density J_{max} a high current flows through the cross-sectional area of the sample S_w (the work area), then, taking into account $Rlin = \rho_g L/S_w$, the dependence of resistivity ρ_{lin} on the volume resistivity of grains ρ_g can be presented as

$$\rho_{lin} = \rho_g S/S_w \quad (14)$$

From (14) follows that a decrease in the value of ρ_{lin} with an increase of J_{max} is a consequence of an increase of area S_w, through which a high electric current flows. At high electric currents the relative work area of a sample S_w/S is

$$S_w/S = \rho_g/\rho_{lin}. \quad (15)$$

The weak dependence of ρ_{lin} on J_{max} above the amplitude current density 1000 A cm^{-2} (Fig. 5) shows that the work area S_w is close to the sample cross-sectional area *S*. In this case, as follows from (15), the resistivity ρ_{lin} is close to the volume resistivity of varistor ceramics grains ρ_g. This region of J_{max} can be used to measure the volume resistivity ρ_g of grains in varistor ceramics [4, 5]. At J_{max} > 1000 A cm^{-2} the resistivity ρ_{lin} limiting the current of intergranular barriers takes values 0.49 – 0.50 Ohm cm. These values correspond to the volume electric resistivity of grains in ZnO based varistor ceramics.

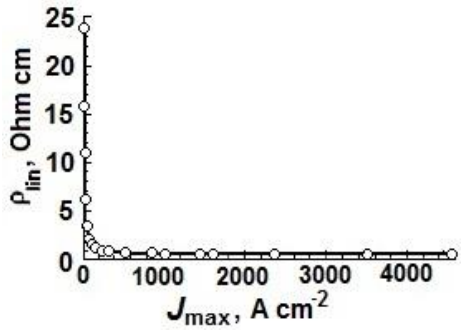

Fig. 5. Dependence of the linear resistivity ρ_{lin} limiting the current of intergranular barriers in ZnO based varistor ceramics on the amplitude density of current pulse J_{max}.

Using ρ_g = 0.495 Ohm cm, the data presented in Fig. 5, and the relation (15), one can obtain the dependence of S_w/S on current pulse amplitude J_{max} (Fig. 6).

The Figs. 5 and 6 are experimental confirmation for computer simulations of electric current transfer in varistor ceramics [9–11]. The authors of these works used an equivalent random grid of nonlinear electrical resistances corresponding to the grain-to-grain contacts in varistor ceramics. The model takes into account the disorder of ceramics caused by the dispersion of grain sizes.

The computer simulation results in the conclusion about the localization of high current in conductive paths connecting the ceramics sample electrodes. This is due to the disorder of ceramics structure and is the reason for uneven distribution of high current in theThe sample. High current flows through the paths with least resistance, the number of which depends on voltage. The formation of such paths is related to the mechanism of deviation from Ohm's law.

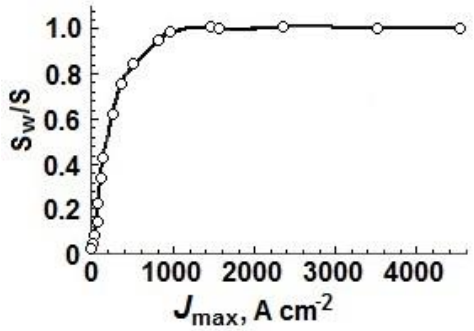

Fig. 6. The relative work area S_w/S of a sample through which high electric current flows as the function of current pulse amplitude J_{max} for ZnO based varistor ceramics

Three mechanisms are known to explain the high nonlinearity of ZnO based ceramics VAC [12–14]. In [12], the nonlinearity is associated with a decrease of the height of energy barriers in electric field and therefore increases in the electric current of above-barrier electron emission. In [13], considering the weak effect of temperature in the section of VAC with high nonlinearity, it is assumed that nonlinearity mechanism is due to tunneling electron emission through the intergranular barrier. In [14], a mechanism of impact ionization was proposed to explain the high nonlinearity of varistor ceramics volt-ampere characteristic.

The work [15] showed that a decrease in height of intergranular barriers cannot be the reason for high nonlinearity of VAC, since for double Schottky barrier in the entire voltage range such decrease does not exceed ~ $0.7k_BT \approx 0.018$ eV (k_B is the Boltzmann constant, T is the temperature). The small decrease in the height of double Schottky barrier is because almost all the voltage applied to the barrier drops in its part biased in the reverse direction.

The most probable mechanism of the high nonlinearity of varistor ceramics VAC is the impact ionization. This is confirmed by the luminescence in a region of intergranular contacts at voltages corresponding to VAC section with a high nonlinearity [14]. The luminescence shows the presence of recombination, as consequence of the hole formation given by impact ionization. A characteristic feature of the impact ionization is the dependence of the electrical breakdown voltage on the band gap energy E_g. For ZnO the band gap is $E_g \sim 3.2$ eV [16]. This value is in accordance with the voltage ~ 3 V, at which high nonlinearity begins, according to the microprobe studies of VAC for grain-to-grain contacts in ZnO varistor ceramics [17]. In this area of VAC the voltage drop on grain contact is close to the value of E_g/e (e is the electron charge). Using this value, it is possible to estimate the voltage applied to the ceramics sample, at which a conductive current path appears between the electrodes. If the grains localized along this path have an average size l_g, then for a sample with thickness L the number of intergranular contacts in current path is L/l_g. Then the voltage U_{th} of reversible electrical breakdown caused by impact ionization is related to the average grain size l_g as

$$U_{th} = E_g L/(el_g) \tag{16}$$

As follows from (16), a voltage to form a current path, along which all intergranular barriers are in the breakdown mode, depends on l_g for this path. For such paths the volume resistance of grains limits the current of intergranular barriers. Since the resistivity of grains ρ_g is small, the conductive paths of current shunt other possible paths between the sample electrodes that contain at least one not punched grain-to-grain barrier.

Since the disorder of varistor ceramics is due to the grain size dispersion, one should expect the presence of conductive current paths with different average size of grains l_b. According to (16), at voltage increasing the conductive paths with greatest values of l_b arise

first. Further, as voltage increases, the paths with smaller values of l_b arise. This explains the uneven distribution of high electric currents over the varistor ceramics sample when J_{max} is less than 1000 A cm^{-2} (Fig. 5). At J_{max} > 1000 A cm^{-2} the weak dependence of ρ_{lin} on J_{max} is because all possible conductive paths of current are switched on and electric current fairly evenly distributed along the cross section of the sample.

The dependence of relative area S_w/S, through which a high current flows, on the amplitude J_{max} for ZnO based varistor ceramics (Fig. 6) is in accordance with the dependence of relative share of current paths on voltage, obtained in [9] by computer simulation.

Using the formation mechanism of conductive paths, it is possible to explain the dependences of ρ_{lin} on average current density J_{av} (Fig. 4). Conductive paths arise when the high ohmic resistance of grain surface layers is shunted by the active and reactive resistances of barriers, which determine the active I_{Rb} and the reactive I_{Cb} current. When ρ_{lin} is measured in a region close to the beginning of current pulse, the contribution of I_{Cb} predominates. This current at a given J_{av} can exceed the I_{Rb} current. As a consequence, one can expect the formation of a greater number of conductive paths than when the active current I_{Rb} is predominating. Therefore, in the region of dependence $\rho_{lin}(J_{av})$ with I_{Cb} predominance, ρ_{lin} takes lower values than in a gentle slop section of this dependence, where I_{Rb} is prevailing.

When all conductive paths of electric current are switched on, the resistivity ρ_{lin} is equal to $\rho_g \sim 0.49 – 0.5$ Ohm cm (Fig. 5). However, according to the Fig. 4, the resistivity ρ_{lin} may be less than the volume resistivity of ZnO grains ρ_g. Such feature can be explained by the edge effects associated with the capacitive current of barriers. These effects can result in the appearance of additional current paths outside the cross-section of a sample with small electrodes S created on varistor surface. As a consequence, using electrodes of area S when measuring ρ_{dif} leads to lower values of ρ_{lin} since the sample cross-sectional area is increased due to the edge effects.

4. Conclusions

A method for measuring the linear resistivity ρ_{lin} limiting the current of intergranular barriers in varistor ceramics is proposed. Grain volume resistivity ρ_g determines ρ_{lin} and is the reason for the decrease of volt-ampere characteristic nonlinearity at high electric currents. Differential resistivity ρ_{dif} is used to measure ρ_{lin}. The value of ρ_{dif} is determined by a program for scanning raster images of voltage and current pulse oscillograms. Both the active and the reactive current of intergranular barriers are taken into account at the measurement.

It has been established that the value of ρ_{lin} is determined by the amplitude of current pulse J_{max}. The sharp dependence of resistivity ρ_{lin} on J_{max} in the range of amplitude current density less than 200 A cm^{-2} indicates a non-uniform distribution of high current over a sample cross section. Electric current flows across the area S_w, which is a part of the sample cross-sectional area S. In this current region, the resistivity ρ_{lin} limiting the current of intergranular barriers is the volume resistivity of grains ρ_g averaged over the area of the electrodes S. In the region J_{max} > 1000 A cm^{-2}, resistivity ρ_{lin} does not depend on J_{max}. That shows the uniform electric current distribution, i.e. $S_w \approx S$. For this current region ρ_{lin} is close to the volume resistivity of grains in ZnO based varistor ceramics $\rho_g \sim 0.49 – 0.50$ Ohm cm.

The reason for the uneven distribution of high currents in varistor ceramics are the disorder associated with the grain size dispersion and the threshold nature of nonlinearity, probably due to impact ionization. A decrease in the nonlinearity of VAC at high electric currents is associated with the appearance of conductive paths between the sample electrodes. Along these paths, all barriers are in the mode of reversible electrical breakdown, and the barrier current is limited by the small volume resistance of grains, which is connected in

series with their contact regions. Disorder caused by the grains size dispersion is the reason for the existence of current paths with different numbers of contacts between the grains. As voltage increases, the current paths with the greatest value of average grain size are switched on first. Further voltage increasing leads to switching on the current paths with a smaller average grain size. This explains the inhomogeneous distribution of high currents over the cross section of varistor. At $J_{max} > 1000$ A cm^{-2} all possible conductive current paths are switched on. Therefore, the resistivity ρ_{lin} is close to the volume resistivity of grains ρ_g.

References

1. **Clarke, D. R.** Varistor ceramics // Journal of the American Ceramic Society. – 1999. – Vol. 82, No. 3. – P. 485 – 502.

2. **Ivon, A. I.** Conductivity of grains in nonlinear oxide ceramics and protective properties of varistors / A. I. Ivon, R. I. Lavrov // Journal of Physics and Electronics. – 2019. – Vol. 27, No. 2. – P. 93 – 98.

3. **Bondarchuk, A. N.** Effects of Sb and Nb dopants on electrical and microstructural properties of low-voltage varistor ceramics based on SnO_2 / A. N. Bondarchuk, A. B. Glot, A. R. Velasco-Rosales // Ceramics International. – 2018. – Vol. 44, No. 7. – P. 7844 – 7850.

4. **Ivon, A. I.** High-current measurement of the grain resistivity in zinc oxide varistor ceramics / A. I. Ivon, R. I. Lavrov, A. B. Glot // Ceramics International. – 2013. – Vol. 39, No 6. – P. 6441 – 6447.

5. **Ivon, A.I.** Grain resistivity in zinc oxide and tin dioxide varistor ceramics / A. I. Ivon, A. B. Glot, R. I. Lavrov, Zhen-Ya Lu // Journal of Alloys and Compounds. – 2014. – Vol. 616. – P. 372 – 377.

6. **Ivon, A.** Web application for high accuracy measurement of volt-ampere characteristics / A. Ivon, V. Istushkin, Yu. Rybka // System technologies. – 2021. – Vol. 133, No. 2. – P. 20 – 25.

7. **Ivon, A.** Software for measuring of differential resistance by scanning of digital images of analog oscillograms / A. Ivon, V. Istushkin // System technologies. – 2021. – Vol. 2(133). – P. 12 – 19.

8. **Ivon, A**. Use of the digital images for measurement of small planar objects geometric parameters with high precision / A. Ivon, V. Istushkin // System technologies. – 2022. – Vol. 138, No. 1. – P. 120 – 126.

9. **Vojta, A.** Influence of microstructural disorder on the current transport behavior of varistor ceramics / A. Vojta, Q. Wen, D. R. Clarke // Computational Materials Science. – 1996. – Vol. 6, No. 1. – P. 51 – 62.

10. **Bartkowiak, M.** Voronoi network model of ZnO varistors with different types of grain boundaries / M. Bartkowiak, G. D. Mahan, F. A. Modine, M. A. Alim, R. Lauf and A. McMillan // Journal of Applied Physics. – 1996. – Vol. 80, No. 11 – P. 6516 – 6522.

11. **Bavelis, K.** Modeling of electrical transport in Zinc Oxide varistors / K. Bavelis, E. Gjonaj and T. Weiland // Advances in Radio Science.– 2014. – Vol. 12. – P. 29 – 34.

12. **Glot, A. B.** A model of non-Ohmic conduction in ZnO varistors // Journal of Materials Science: Materials in Electronics. – 2006. – Vol. 17, No. 9. – P. 755 – 765.

13. **Eda, R.** Conduction mechanism of non-Ohmic zinc oxide ceramics // Journal of Applied Physics. – 1978. – Vol. 49, No. 5. – P. 2964 – 2972.

14. **Pike, G. E.** Electroluminescence in ZnO varistors: Evidence for hole contributions to the breakdown mechanism / G. E. Pike, S. R. Kurtz, P. L. Gourley, Y. R. Philipp and L. M. Levinson // Journal of Applied Physics. – 1985. – Vol. 57, No. 12. – P. 5512 – 5518.

15. **Ivon, A. I.** Volt-ampere characteristics of the double Shottky barrier // Journal of Physics and Electronics. – 2021. – Vol. 29, No. 1. – P. 91 – 98.

16. **Srikant, V.** On the optical band gap of zinc oxide / V. Srikant and D. R. Clarke // Journal of Applied Physics. – 1998. – Vol. 83, No. 10. – P. 5447 – 5451.

17. **Olsson, E.** Characteristics of individual interfacial barriers in a ZnO varistor material. / E. Olsson, G. L. Dunlop // Journal of Applied Physics. – 1989. – Vol. 66, No. 8. – P. 3666 – 3675.